Bull. Astr. Soc. India (1993) **21**, 587-590

Balloon-borne far-infrared mapping of Galactic star forming regions

B. Das[1], S. K. Ghosh[1], T. N. Rengarajan[1], R. P. Verma[1],
K. V. K. Iyengar[2] and S. N. Tandon[3]
[1]*Tata Institute of Fundamental Research, Bombay 400 005*
[2]*Indian Institute of Astrophysics, Bangalore 560 034*
[3]*Inter-University Centre for Astronomy and Astrophysics, Pune 411 007*

Abstract. Large angular areas (> 500 sq arcmin each) covering the three Galactic star forming regions (NGC 2024, OMC-1/OMC-2, and IRAS 06058 + 2138 and its neighbourhood) have been mapped in two FIR bands (58 and 150 μm) with ≈ 1′.5 resolution using the TIFR 100 cm balloon-borne telescope. The resulting intensity maps as well as colour temperature and optical depth (for NGC 2024 only) maps are presented and their implications are discussed.

Key words : star formation—far-infrared observation

1. Observation

With the aim of studying interstellar dust distribution and energetics of Galactic star forming regions, three regions have been studied. Two of these, viz., NGC 2024 and Orion Molecular Cloud (OMC), are known to be undergoing star formation and the third contains relatively weaker IRAS point sources (IRAS 06056 + 2131, 06058 + 2138 and 06061 + 2151) with a similar rising infrared spectrum. Large angular areas (> 500 sq arcmin each) centred on these sources have been mapped simultaneously in two far-infrared bands centred at 58 μm and 150 μm using the TIFR 100 cm balloon-borne telescope with 2′.4 beam (FWHM). The telescope, FIR photometer as well as data processing details can be found elsewhere (Ghosh *et al.* 1992).

The maps presented here have angular resolution of 1′.5 which is achieved by using a maximum entropy deconvolution procedure. (This achieved resolution is sub-optimal due to a mechanical damage to the telescope aspect sensor). Angular regions mapped centering around these programme sources are listed in table 1.

IRAS pointed observations relevant to NGC 2024 and OMC regions (for 60 and 100 μm bands) have been processed for improving angular resolution by a self adaptive maximum entropy deconvolution scheme (Ghosh *et al.* 1993). The resulting resolutions of these maps are inferior to the resolution in the maps obtained from the balloon-borne data.

2. Results

Figures 1a and 1b show intensity maps of NGC 2024 for 58 μm and 150 μm respectively superposed with corresponding IRAS maps for 60 and 100 μm in dotted lines. The dust temperature and optical depth (τ_{150}) are computed from 58 μm and 150 μm intensity maps assuming an emissivity law $\varepsilon_\lambda \propto \lambda^{-1}$. Both of these are presented in figures 1c and 1d respectively. Similarly, 58 μm and 150 μm intensity maps of OMC-2/OMC-1 are presented in figures 2a and 2b respectively, and the region around IRAS 06058 + 2138 shown in

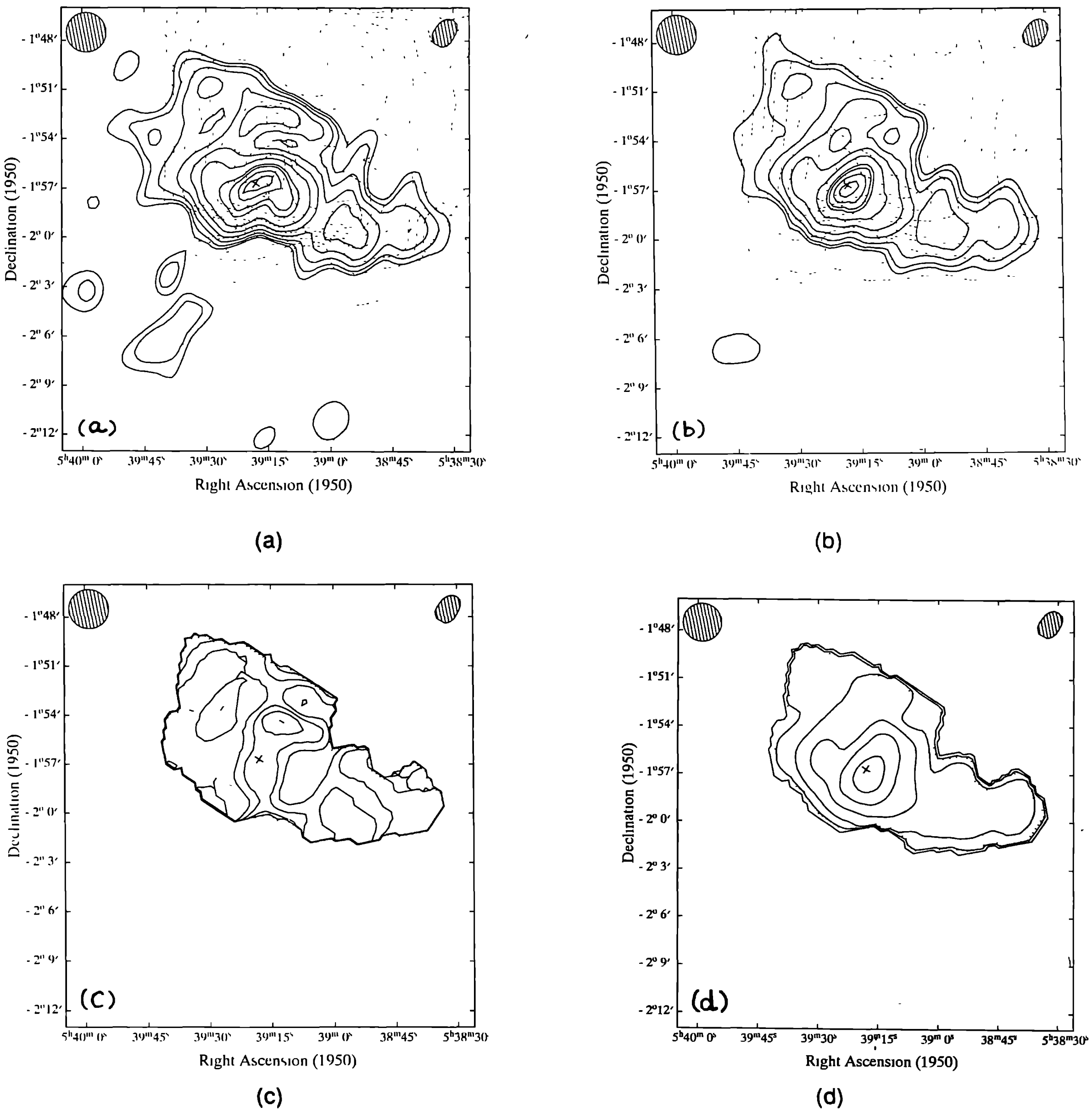

Figure 1. FIR intensity contours of NGC 2024, plotted at 90, 70, 50, 40, 20, 10, 5, 2.5, 1.25, and 0.62 percent levels of the peak. Shaded circle is the telescope beam and the ellipse is the map resolution. (a) 58 μm map, peak = 1.11×10^4 Jy/sq arcmin, (b) 150 μm, peak = 9.56×10^3 Jy/sq arcmin, (c) The temperature contours at values 60, 50, 45, 40 and 35 K. (d) The optical depth (τ_{150}) contours for 150 μm at values 4.39E-2, 1.46E-2, 4.88E-3, 1.63E-3 and 5.42E-4.

figures 3a and 3b. Flux densities, dust temperatures and FIR luminosities for the major peaks in these maps are listed in table 1.

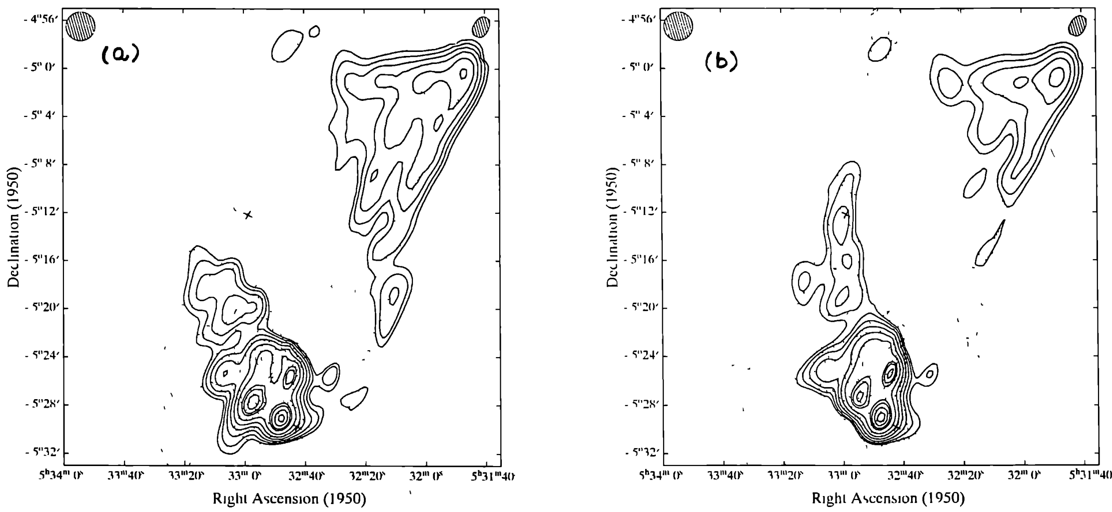

(a) (b)

Figure 2. FIR intensity maps of OMC-2/OMC-1 complex. Contour levels are at 90, 70, 50, 40, 20, 10, 5, 2.5, 1.25, 0.62, 0.31, and 0.16 percent of the peak. (a) 58 μm map, peak = 2.89×10^4 Jy/sq arcmin and (b) 150 μm map, peak = 1.67×10^4 Jy/sq arcmin.

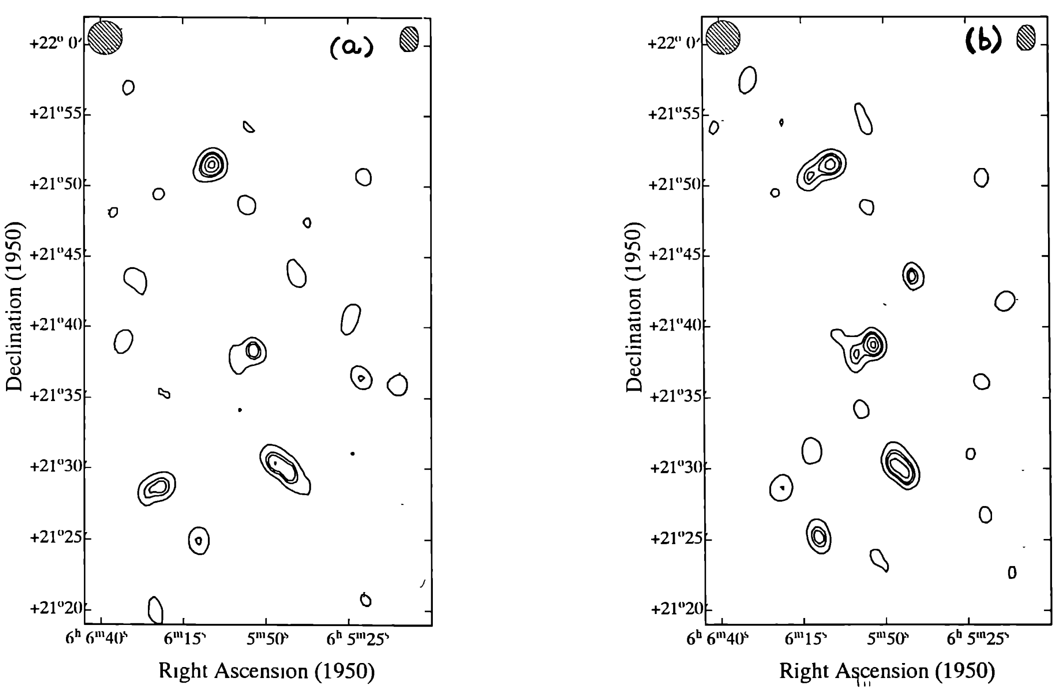

(a) (b)

Figure 3. FIR intensity maps of the region centred around IRAS 06058 + 2138. Contours are at 90, 70, 50, 40, and 20 percent of the peak. (a) 58 μm map, peak = 5.89×10^2 Jy/sq arcmin and (b) 150 μm map, peak = 6.78×10^2 Jy/sq arcmin.

Table 1. Details of the programme sources

Source Name	D^* (pc)	Area	I.F.D.† (Jy) 58 μm	150 μm	Dust Temp K	Luminosity $L_\odot$
NGC 2024	450	23′ × 21′	3.3×10^4	2.7×10^4	43	1.3×10^4
OMC-2	500	25′ × 35′	2.6×10^2	1.8×10^3	26	3.2×10^2
OMC-1	500	25′ × 35′	8.25×10^4	4.0×10^4	52	3.1×10^4
IRAS 06056 + 2131	800	21′ × 41′	9.8×10^2	1.2×10^3	38	4.1×10^2
IRAS 06058 + 2138	800	21′ × 41′	6.7×10^2	9.2×10^2	37	3.0×10^2
IRAS 06061 + 2151	800	21′ × 41′	8.3×10^2	1.4×10^3	35	4.1×10^2

*Distance from Dame *et al.* 1987.
†Integrated flux density within 3′ diameter circle around peak.

3. Discussion

The exciting star of NGC 2024 is estimated (from L_{FIR}) to be a ZAMS B0.5 type star. The dust temperature in the central region is 66 K and gradually falls to 35 K at about 0.5 pc away. Radio molecular line (^{13}CO) measurement gives the column density $N(H_2) \approx 10^{23}$ cm^{-2} and the gas temperature ≈ 100 K heated by a shock wave (Graf *et al.* 1993).

The FIR source OMC-2, first identified by Gatley *et al.* (1974) from their CO measurement, is found to be cold ($T_d \approx 25$ K), of low luminosity (≈ 300 $L_\odot$) and low gas mass (≈ 150 $M_\odot$, Thronson *et al.* 1978). No free-free emission in radio wavelength has been detected (Gatley *et al.* 1974) from this region which suggests that the exciting source is a pre-main sequence star of type A or later. External heating of this region by OMC-1 can be ruled out from simple geometric considerations.

The three isolated sources in figure 3, corresponding to IRAS point sources IRAS 06056 + 2131, 06058 + 2138 & 06061 + 2151 contain fairly warm dust ($T_d \approx 35$ K). The lack of any nearby energy source rules out the possibility of their being dense clumps heated externally. Further radio continuum and radio molecular (CO) observations are needed to decide about the energy sources.

References

Dame T. M., Ungerechts H., Cohen R. S., De Gues E. J., Grenier I. A., May J., Murphy D. C., Nyman L. A., Thaddeus P., 1987, ApJ, 322, 706.

Gatley I., Becklin E. E., Mathews K., Neugebauer G., Penston M. V., Scoville N., 1974, ApJ, 191, L121.

Ghosh S. K., Bisht R. S., Iyengar K. V. K., Rengarajan T. N., Tandon S. N., Verma R. P., 1992, ApJ, 391, 111.

Ghosh S. K., Verma R. P., Rengarajan T. N., Das B., Saraiya H. T., 1993, ApJS, 86, 401.

Graf U. U., Eckart A., Genzel R., Harris A. I., Poglitsch A., Russel A. P. G., Stutzki J., 1993, ApJ, 405, 249.

Thronson H. A., Harper D. A., Keene J., Loewenstien R. F., Moseley H., Telesco C. M., 1978, AJ, 83, 492.